Dynamics and superconductivity in compressed lanthanum superhydride

Hanyu Liu,[1,*] Ivan I. Naumov,[1] Zachary M. Geballe,[1] Maddury Somayazulu,[2] John S. Tse,[3,†] and Russell J. Hemley[2,‡]

[1]*Geophysical Laboratory, Carnegie Institution of Washington, Washington, DC 20015, USA*

[2]*Institute of Materials Science and Department of Civil and Environmental Engineering, The George Washington University, Washington, DC 20052, USA*

[3]*Department of Physics, University of Saskatchewan, Saskatoon Canada, S7N5E2*

Recent computational studies have predicted that rare-earth superhydrides are promising high-temperature superconductors. Of these phases having very high hydrogen content (XH_n, $n > 6$, where X is the rare-earth atom) a cubic phase of lanthanum hydride, recently synthesized at 170 GPa and identified as $LaH_{10\pm x}$, is in good agreement with theoretical predictions. The experiments found that the stability of the phase extended to lower pressure and a distorted form was found on decompression. Here we examine the nuclear quantum effects and anharmonic dynamics on LaH_{10}, including the behavior of the hydrogen sublattice in comparison with the predicted atomic metallic hydrogen at higher pressure. We also examine the vibrational dynamics and electronic properties of a distorted lower pressure phase of LaH_{10} and find that superconducting T_c decreases relative to cubic but remains relatively high (i.e., 229–245 K).

I. INTRODUCTION

Hydrogen and hydrogen-rich materials are of great current interest in achieving very high-temperature superconductivity through the conventional theory of phonon-mediated superconductivity due to the high average phonon frequencies of these materials, although the details are more complicated [1–6]. As such, metallic hydrogen-dominated compounds could potentially exhibit high superconducting transition temperatures T_c. Several such compounds with variable T_c have been produced in the laboratory (e.g., Refs. [7–12]). Among them, compressed H_2S is thought to be the most notable as it may become a superconductor with a record T_c of 203 K at 150 GPa [9,13]. Theoretical studies suggested this high superconducting phase is H_3S [14–17]. It is clear that one should look for systems with the highest possible hydrogen content. Later, we systematically performed structure search in the La-H and Y-H systems. We predicted several hydrogen-rich compounds, including LaH_{10} and YH_{10} in a *fcc* lattice, in which 32-atom hydrogen cages enclathrate the La and Y atoms in the structure [18]. Both phases are predicted to have superconducting transition temperatures near room temperature: $\sim$275 K at 210 GPa for LaH_{10} and $\sim$305 K at 250 GPa in YH_{10}, in good agreement with the calculations reported by another theoretical group [19].

In addition to being more accessible experimentally than pure atomic metallic hydrogen, the structure of such hydrogen-dominated compounds (or superhydrides) can be determined with a much higher degree of definiteness, especially with the use of x-ray diffraction to determine the sublattice associated with a heavier component. The predicted *fcc*-LaH_{10} phase was recently synthesized at pressures above 170 GPa [20]. The experiments found that the stability of the phase extended to somewhat lower pressure than was originally predicted, and the cubic phase was found to undergo a distorted form on decompression below 170 GPa. The previous calculations show that the *fcc*-LaH_{10} is dynamically unstable below 210 GPa [18]. However, the experiment found it is stable at 170 GPa, a discrepancy that may arise from anharmonic effects that are not accounted for in previous simulations.

Here we study the phase stability and superconductivity of LaH_{10} with special emphasis on nuclear dynamical effects. We show that prediction for the LaH_{10} phase stability requires taking into account nuclear vibrations, both classical and quantum. These effects also lead to a sublattice melting associated with H atoms, and the corresponding melting temperature, T_{ms}, increases with pressure. This temperature, however, is relatively high ($\sim$1000 K), i.e., well above the predicted superconducting transition temperature and the experimental synthesis of Ref. [20]. As the pressure decreases, *fcc*-LaH_{10} undergoes a structural transformation to a lower symmetry $C2/m$-LaH_{10} phase, which still exhibits a relatively high T_c of $\sim$240 K. These studies can be extended to other hydrogen-dominated materials and pure hydrogen, since they have similar light element environments, including H-H distances and coordination.

II. RESULTS AND DISCUSSION

We begin by examining the effects of thermal anharmonic vibrations and quantum motions on the stability of the higher symmetry (*fcc*) LaH_{10} phase to lower pressures. For this purpose, we performed first-principles classical and path integral molecular dynamics simulations; see below and Supplemental

*Corresponding author: hanyuliu801@gmail.com

†john.tse@usask.ca

‡rhemley@email.gwu.edu
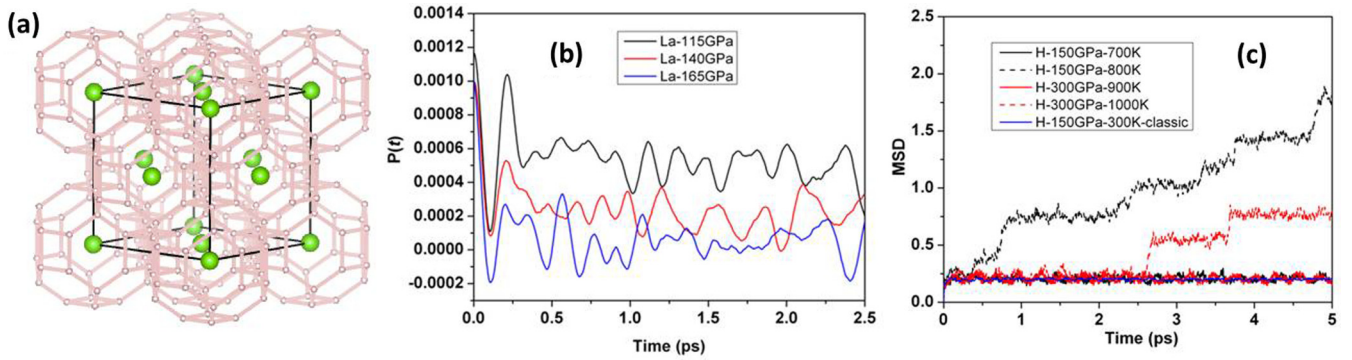
FIG. 1. (a) Static structure of fcc-LaH$_{10}$. (b) Position correlation functions of LaH$_{10}$ at 115, 140, and 165 GPa and 300 K. (c) Mean-squared displacement (MSD) of H atoms for fcc-LaH$_{10}$ 150 and 300 GPa, and 300–1000 K.

Material, Ref. [21] for additional details. Classical molecular dynamic simulations at 115, 140, and 165 GPa were performed using a supercell consisting of 352 atoms (32 La and 320 H atoms). The atomic dynamics were analyzed *via* the calculation of the position correlation function, $p(t) = \langle (r_i(t + t_0) - R_i^0) \bullet (r_i(t_0) - R_i^0) \rangle$, where $\boldsymbol{r}_i$ is the temporal position of the *i-th* atom and $\boldsymbol{R}^0_i$ is the initial position of that atom in the starting structure. The angular brackets denote thermal averaging that, in practice, is evaluated as the average over many time origins t_0. At long time, the positional displacements would become uncorrelated, therefore, $p(t) = \langle (r_i(t + t_0) - R_i^0) \bullet (r_i(t_0) - R_i^0) \rangle \rightarrow \langle r_i - R_i^0 \rangle^2$. That is, if all atoms vibrate about the initial lattice sites, then $\langle r_i - R_i^0 \rangle = 0$, and $p(t) \rightarrow 0$ as $t \rightarrow \infty$ indicating the structure is dynamically stable. The position correlation functions in Fig. 1 show the La atoms displaced far away from the ideal fcc positions, therefore, the fcc-LaH$_{10}$ is not stable at room temperature and 115 and 140 GPa, However, the structure becomes stable above 140 GPa, in agreement the experimental observation [20].

To investigate nuclear quantum effects, we performed path integral molecular dynamic simulations of fcc-LaH$_{10}$ at 150 GPa and 300 GPa. The quantum motion of each H atom is simulated by a ring polymer with 16 beads [21]. We found that the inclusion of the quantum effects was similar to the results obtained from classical molecular dynamic simulation (Fig. 1), and the La and H still occupied the respective fcc positions at 150 GPa and 300 K. The calculated average root mean vibration amplitude $\sqrt{(\langle u \rangle^2)}$ of H atoms are respectively, 0.20 and 0.23 Å, from classical and quantum molecular dynamic simulations at 150 GPa and 300 K. In the case of quantum simulation, the amplitude exceeds ∼20% of the H-H separation, which is close to the Lindemann criterion for melting. This value is much larger than those reported for the molecular $C2/c$, $Cmca$-12, and $Pbcn$ phases of pure hydrogen at 200 K (predicted values of 0.21, 0.14, and 0.13, respectively) [22] and is less than that in helium (28%) [23]. Furthermore, we have investigated the trajectories of La and H atoms at different temperatures, where the trajectories of hydrogen atoms represented by different colors as shown in Fig. 2(b). It is clearly seen some hydrogen atoms can diffuse in the lattice (Fig. 2), not unlike that found in water ice at megabar pressures (e.g., Ref. [24]). Moreover, we found

that the hydrogen atoms become diffusive at 800 K and 150 GPa and 1000 K and 300 GPa, indicating the T_{ms} increases with pressure. This observation suggests that fcc-LaH$_{10}$ may become a superionic phase under high pressure.

We now compare the H substructure of fcc LaH$_{10}$ with the atomic $I4_1/amd$ (Cs-IV) [25,26] and molecular $C2/c$ [25] phases of solid hydrogen. The hydrogen atoms in fcc-LaH$_{10}$ and $I4_1/amd$ hydrogen have a similar chemical bonding environment (Figs. 3 and S1) in the sense that the H atoms have four nearest neighbors forming "sp^3" type bonding [21]. The systems also share similar features in the projected density of states (PDOS) near the Fermi energy (Fig. S2). In both systems, the H-s orbitals contributed much more than the p orbitals to the electronic density of states (DOS). The pressure dependence of the H-H distances in LaH$_{10}$ and Cs-IV exhibit similar trends (Fig. S3). The similar chemical interaction between the H atoms is highlighted from the contour plots of the electron localization functions shown in Fig. 3.

In the harmonic approximation, fcc-LaH$_{10}$ is dynamically unstable below 210 GPa [18]. The total energy decreases upon small atomic displacements (Fig. S4). At this pressure, after full geometry optimization, a slightly distorted $C2/m$ structure is found. We computed the phonon band structure of the $C2/m$ phase at 200 GPa. The results show no imaginary mode in the BZ, indicating the phase is a dynamically stable structure as shown in Fig. 4. As in fcc-LaH$_{10}$, there is no clear
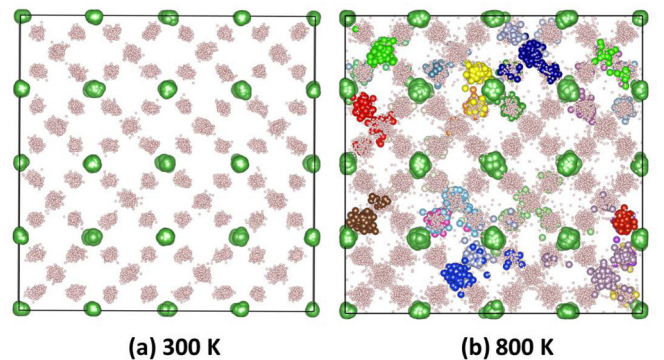
FIG. 2. The trajectories of La (green spheres) and H (pink spheres) atoms at (a) 300 K and (b) 800 K simulations at 150 GPa. (b) The trajectories of some H atoms are marked by different colors.
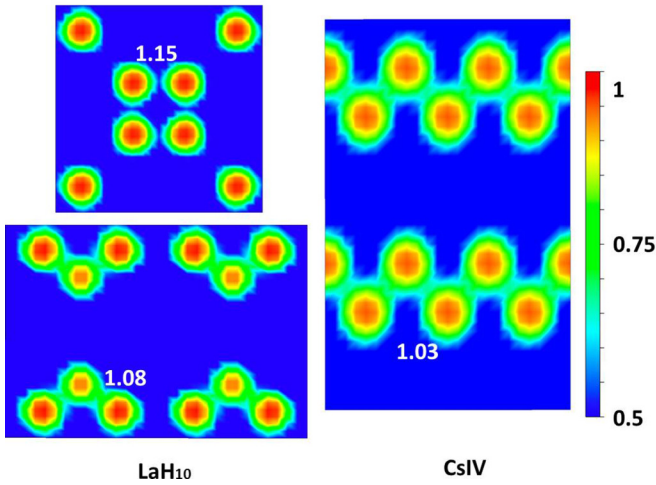
FIG. 3. Electron localization function (ELF) of cubic LaH_{10} and Cs-IV-type atomic hydrogen at 200 GPa.

separation H-H stretching and bending vibrations in the calculated phonon band structure and projected vibration density of states (PVDOS) [3]. The PVDOS shows that La vibrations dominate below $250 \, cm^{-1}$. The absence of the distinct H-H stretch vibrations and their strong mixing with the vibrations have been shown to be a unique feature in superhydrides [3]. It would be of interest to extend these calculations for this and other lower symmetry structures to include nuclear quantum effects as for cubic LaH_{10} discussed above. It is interesting to note that the cutoff frequency at $2200 \, cm^{-1}$ is much lower than that of the molecular hydrogen phases at these pressures, e.g., the *Cmca*-4 phase of hydrogen (Fig. S5).

Previously, we found the electron-phonon coupling $\lambda = 2.2$ for *fcc*-LaH_{10} [18]. The T_c was estimated from $\alpha^2 F(\omega)$ by numerically solving the Eliashberg equations [27,28], and calculations with $\mu^* = 0.1-0.13$ gave a predicted T_c of 257–274 K (at 250 GPa) [18]. Turning to the $C2/m$ structure, integration of $\alpha^2 F(\omega)$ shows that 76% of the electron-phonon coupling is derived from H-H vibrations above $250 \, cm^{-1}$ (Fig. 4). We find $\lambda = 3.57$, which is very large but comparable to that calculated for H_3S [14]. Using this value for λ, the calculated logarithmic average of phonon frequency
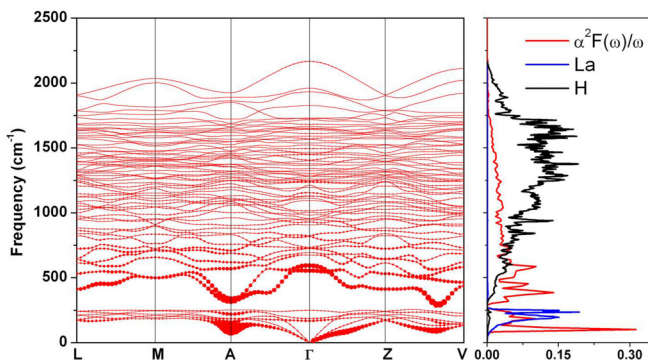
FIG. 4. The calculated phonon and electron-phonon coupling spectral function for the $C2/m$ structure of LaH_{10} at 200 GPa. The size of the red solid circles indicates the electron-phonon coupling strength.

$\omega_{log} = 733 \, K$, and the density of electronic states at the Fermi level, we compute T_c of 200 K for the $C2/m$ structure at 200 GPa with the McMillan formula. The corresponding range of T_c for $\mu^* = 0.1-0.13$ is 245–229 K. These numbers are within range computed from the directly solving Eliashberg equation using $\alpha^2 F(\omega)$, i.e, $T_c = 238 \, K$. For the Cs-IV structure of solid hydrogen, the calculations give $\lambda = 3.45$ and $\omega_{log} = 1225 \, K$, which in turn give a T_c from the McMillan equation of $\sim$370 K (at 300 GPa).

To further understand which parameters contribute most to the electron-phonon coupling, we used a simplified expression for λ in the McMillan-Hopfield form

$$\lambda = \frac{N(E_f)\langle I^2 \rangle}{M \langle \omega^2 \rangle},$$

where M is the atomic mass, $\langle I^2 \rangle$ is the square of the electron-ion matrix element at the Fermi level, and $\langle \omega^2 \rangle$ is the averaged square of phonon frequency. The electron density of states $N(E_f)$ in the Cs-IV phase is 0.49 states/Ry/atom at 300 GPa, roughly half that in LaH_{10} at 200 GPa (0.89 states/Ry/atom), which provides an explanation for the larger electron-phonon coupling strength of LaH_{10} relative to Cs-IV-type hydrogen. The structural distortion from the cubic LaH_{10} decreases the T_c of the $C2/m$ phase somewhat but this is still predicted to remain above 200 K at these pressures. We point out that additional lower symmetry phases in the La-H were found on decompression of *fcc*-LaH_{10} [20]; it is possible that these phases are also superconductors, possibly with still lower transition temperatures.

III. CONCLUSIONS

In summary, we demonstrate that both thermal and quantum effects play crucial roles in determining the stability of *fcc*-LaH_{10}, a potential very high-T_c superconductor and the most hydrogen-rich metallic compound synthesized to date. The dynamical effects diminish the orientational character of the chemical bonds and stabilize the higher symmetry (*fcc*) phase at lower pressures, in agreement with the recent experiments. The T_c of LaH_{10} is predicted to decrease in the lower symmetry $C2/m$ phase is less than that of cubic but is still predicted to be high (e.g., 229–245 K) and lower pressure superconducting phases are possible in the La-H system. Comparing LaH_{10} with the Cs-IV phase of solid hydrogen, we found that in both systems the hydrogen atoms have similar chemical bonding environments. Moreover, the melting temperature of the H sublattice in LaH_{10} increases with pressure, similar to the bulk melting curve predicted for the Cs-IV phase. Such studies can be extended to other rare-earth superhydrides that are likely to exhibit similar unprecedented dynamical and electronic properties.

IV. METHODS

The phonon band structure and electron-phonon coupling parameters were computed within the density functional perturbation theory using the Quantum-ESPRESSO package [29]. Ultrasoft pseudopotentials for $La(5s^2 \, 5p^6 \, 5d^1 \, 6s^2)$ and $H \, (1s^1)$ were used with a kinetic energy cutoff of 60 Ry. To validate the pseudopotentials, we compared the

equation of state of fcc-LaH$_{10}$ computed from Projector augmented Wave (PAW) potentials [30,31] and ultrasoft pseudopotentials to full-potential calculations. To validate these calculations, we calculated the equation of states for fcc-LaH$_{10}$ using different potentials [Fig. S6]. Additionally, we recalculated the convex-hull on La-H at 200 GPa with and without zero-point energy as shown in Fig. S7 using the global structure prediction method CALYPSO [32,33]. In agreement with our recent experiments, these calculations clearly validate the observed stability of LaH$_{10}$ to be derived from the zero point energy. To calibrate the accuracy of the electron-phonon coupling calculations, we computed the T_c of Cs-IV phase of solid hydrogen at 500 GPa, since this quantity has already been reported in previous work [34,35].

[1] N. W. Ashcroft, Phys. Rev. Lett **21**, 1748 (1968).

[2] N. W. Ashcroft, Phys. Rev. Lett. **92**, 187002 (2004).

[3] K. Tanaka, J. S. Tse, and H. Liu, Phys. Rev. B **96**, 100502 (2017).

[4] L. Zhang, Y. Wang, J. Lv, and Y. Ma, Nature Mater. Rev. **2**, 17005 (2017).

[5] D. Duan, Y. Liu, Y. Ma, Z. Shao, B. Liu, and T. Cui, Natl. Sci. Rev. **4**, 121 (2017).

[6] H. Wang, X. Li, G. Gao, Y. Li, and Y. Ma, Comput. Mol. Sci. **8**, e1330 (2017).

[7] G. Gao, A. R. Oganov, A. Bergara, M. Martinez-Canales, T. Cui, T. Iitaka, Y. Ma, and G. Zou, Phys. Rev. Lett. **101**, 107002 (2008).

[8] M. Eremets, I. Trojan, S. Medvedev, J. Tse, and Y. Yao, Science **319**, 1506 (2008).

[9] A. P. Drozdov, M. I. Eremets, I. A. Troyan, V. Ksenofontov, and S. I. Shylin, Nature (London) **525**, 73 (2015).

[10] E. Zurek, R. Hoffmann, N. W. Ashcroft, A. R. Oganov, and A. O. Lyakhov, Proc. Natl. Acad. Sci. USA **106**, 17640 (2009).

[11] X. Chen, V. V. Struzhkin, Y. Song, A. F. Goncharov, M. Ahart, Z. Liu, H. Mao, and R. J. Hemley, Proc. Natl. Acad. Sci. USA **105**, 20 (2008).

[12] X. J. Chen, J. L. Wang, V. V. Struzhkin, H. K. Mao, R. J. Hemley, and H. Q. Lin, Phys. Rev. Lett. **101**, 077002 (2008).

[13] Y. Li, J. Hao, H. Liu, Y. Li, and Y. Ma, J. Chem. Phys. **140**, 174712 (2014).

[14] D. Duan, Y. Liu, F. Tian, D. Li, X. Huang, Z. Zhao, H. Yu, B. Liu, W. Tian, and T. Cui, Sci. Rep. **4**, 6968 (2014).

[15] A. P. Durajski, R. Szcześniak, and L. Pietronero, Ann. Phys. (Berlin) **528**, 358 (2015).

[16] I. Errea, M. Calandra, C. J. Pickard, J. R. Nelson, R. J. Needs, Y. Li, H. Liu, Y. Zhang, Y. Ma, and F. Mauri, Phys. Rev. Lett. **114**, 157004 (2015).

[17] Y. Li, L. Wang, H. Liu, Y. Zhang, J. Hao, C. J. Pickard, J. R. Nelson, R. J. Needs, W. Li, Y. Huang, I. Errea, M. Calandra, F. Mauri, and Y. Ma, Phys. Rev. B **93**, 020103 (2016).

[18] H. Liu, I. I. Naumov, R. Hoffmann, N. Ashcroft, and R. J. Hemley, Proc. Nati. Acad. Sci. USA **114**, 6990 (2017).

[19] F. Peng, Y. Sun, C. J. Pickard, R. J. Needs, Q. Wu, and Y. Ma, Phys. Rev. Lett. **119**, 107001 (2017). Some similar results in this reference have been previously reported in Walter Kohn Prize lecture in 18th Total Energy Workshop, ICTP, Trieste (Italy), January 13th, 2017.

[20] Z. M. Geballe, H. Liu, A. K. Mishra, M. Ahart, M. Somayazulu, Y. Meng, M. Baldini, and R. J. Hemley, Angew. Chem. Int. Ed. **57**, 688 (2017).

[21] See Supplemental Material at http://link.aps.org/supplemental/10.1103/PhysRevB.98.100102 for more computational details on the structure prediction and ab initio molecular dynamics simulations as well as additional results.

[22] V. Labet, P. Gonzalez-Morelos, R. Hoffmann, and N. W. Ashcroft, J. Chem. Phys. **136**, 074501 (2012).

[23] M. A. Morales, J. M. McMahon, C. Pierleoni, and D. M. Ceperley, Phys. Rev. B **87**, 184107 (2013).

[24] M. Millot, S. Hamel, J. R. Rygg, P. M. Celliers, G. W. Collins, F. Coppari, D. E. Fratanduono, R. Jeanloz, D. C. Swift, and J. H. Eggert, Nat. Phys. **14**, 297 (2018).

[25] C. J. Pickard and R. J. Needs, Nat. Phys. **3**, 473 (2007).

[26] H. Liu, H. Wang, and Y. Ma, J. Phys. Chem. C **116**, 9221 (2012).

[27] A. P. Durajski, Sci. Rep. **6**, 38570 (2016).

[28] A. P. Durajski, Sci. Rep. **8**, 6037 (2018).

[29] P. Giannozzi, S. Baroni1, N. Bonini, M. Calandra, R. Car, C. Cavazzoni, D. Ceresoli, G. L Chiarotti, M. Cococcioni, I. Dabo, A. D. Corso, S. de Gironcoli, S. Fabris, G. Fratesi, R. Gebauer, U. Gerstmann, C. Gougoussis, A. Kokalj, M. Lazzeri, L. Martin-Samos1, N. Marzari, F. Mauri, R. Mazzarello, S. Paolini, A. Pasquarello, L. Paulatto, C. Sbraccia, S. Scandolo, G. Sclauzero, A. P. Seitsonen, A. Smogunov, P. Umari, and R. M. Wentzcovitch, J. Phys. Condens. Matter **21**, 395502 (2009).

[30] G. Kresse and D. Joubert, Phys. Rev. B **59**, 1758 (1999).

[31] G. Kresse and J. Furthmüller, Phys. Rev. B **54**, 11169 (1996).

[32] Y. Wang, J. Lv, L. Zhu, and Y. Ma, Comp. Phys. Commun. **183**, 2063 (2012).

[33] Y. Wang, J. Lv, L. Zhu, and Y. Ma, Phys. Rev. B **82**, 094116 (2010).

[34] J. M. McMahon and D. M. Ceperley, Phys. Rev. B **84**, 144515 (2011).

[35] T. Ishikawa, H. Nagara, T. Oda, N. Suzuki, and K. Shimizu, J. Phys.: Conf. Ser. **950**, 042009 (2017).